

Rotation of the linear-polarization plane of transmitted and reflected light by single- and few-layer graphene

T. Jiang,¹ D. Emerson,² K. Twarowski,² D. Finkenstadt,³ and J. Therrien^{2,*}

¹*Department of Physics, University of Massachusetts–Lowell, Lowell, Massachusetts 01854, USA*

²*Electrical and Computer Engineering Department, University of Massachusetts–Lowell, Lowell, Massachusetts 01854, USA*

³*Physics Department, US Naval Academy, Annapolis, Maryland 21402, USA*

(Received 28 July 2010; published 15 December 2010)

Transmission and reflection measurements performed on single- and few-layer graphene indicate the presence of circular dichroism (CD). Surface roughness appears to moderate the effect with ultraflat graphene on mica not showing CD. Application of an external magnetic field had no effect, ruling out any contribution from spin polarization. Symmetry breaking of the graphene lattice due to a soft shear mode in the graphene sheet is believed to be the origin of the requisite asymmetry for this effect to occur.

DOI: [10.1103/PhysRevB.82.235430](https://doi.org/10.1103/PhysRevB.82.235430)

PACS number(s): 78.20.Ek, 78.66.Tr, 78.67.Pt

I. INTRODUCTION

A large number of the applications for graphene have focused on the transport properties.^{1–5} Devices exploiting the mechanical qualities^{6,7} of graphene are not much further behind in development. It is a material of interest for nanocomposites as well.⁸ The potential for chemical⁹ and biological sensors^{10,11} is being explored. Systems that exploit the optical properties,¹² in particular, the transparency, in conjunction with other properties may be relative late comers but they will likely see widespread use. To date, there have been a number of studies that have addressed optical transmission in graphene,^{13–17} however none have investigated optical activity.

Optical activity in materials occurs due to one of two effects, both involving the breaking of mirror symmetry. In the most common instance, a material contains an arrangement of bonds that form an asymmetric structure. Good examples of this are simple sugars, such as glucose and fructose, whose solutions rotate the plane of polarization of light in opposite directions; the difference being the helicity of the molecules.¹⁸ The second method for inducing optical activity is by magnetizing the sample to obtain spin polarization in the electrons.¹⁹

When considering graphene, neither of these conditions would appear likely. The symmetry of the lattice of idealized graphene will not induce rotation in polarization. Additionally, to date there have not been any reports of ferromagnetism being observed in exfoliated graphene. In contrast to these expectations, we report here the observation of optical chirality in single- and few-layer graphene prepared via mechanical exfoliation. Graphene was found to be visible by eye when placed between crossed linear polarizers on silicon covered with various thicknesses of silicon dioxide and on glass. Quantitative values for the circular dichroism (CD) were determined for graphene on glass for thicknesses from one to seven layers. The CD was found to increase for the first three layers and then remain relatively unchanged as thickness increases. Given that the first few layers are most affected by substrate surface roughness, we investigate strain as a means to induce shear and optical chirality, as it would seem to occur naturally due to strain during exfoliation. The

experimental observation of chirality offers then, a potential method for identifying strained versus unstrained graphene samples.

II. EXPERIMENT

Graphene samples were prepared via the mechanical exfoliation “rubbing” method, where the highly oriented pyrolytic graphite (HOPG) is cleaned first with application and subsequent peeling off of tape. This surface is then pressed against the substrate of interest to transfer the graphene. One advantage of this approach is the minimization of adhesive residues.²⁰ Samples were characterized by atomic force microscopy (AFM) as well as optical absorption of unpolarized light for the samples on glass. In the case of the samples on glass, thicknesses were determined by measurement of the percent absorption relative to the adjacent substrate, where it has been shown that each layer of graphene accounts for 2.3% of the absorbed light.¹⁴ Micro-Raman measurements were performed on samples on both glass and silicon to corroborate the thickness measurements²¹ obtained by AFM and optical absorption.

Polarization and CD measurements were performed in an Olympus CX41 microscope using a DP-71 charge coupled device camera. Samples with an opaque substrate were observed with linearly polarized illumination. For images taken with crossed polarizers, a second polarizer (analyzer) oriented to block the reflected light from the sample was placed before the camera. Images of the same substrates taken with circularly polarized light were obtained by placing a properly oriented $\frac{1}{4}$ wave plate before the objective lens with a linear polarizer placed at the light source. In this configuration, the $\frac{1}{4}$ wave plate produces circularly polarized light from the linearly polarized light before reaching the sample but on return, the light only passes through the $\frac{1}{4}$ wave plate and no polarizer, thus preserving the information about the sample’s interaction with the circularly polarized light. Samples on glass were observed with illumination through the substrate. Linearly and circularly polarized illumination was generated using the linear polarizer and $\frac{1}{4}$ wave plate as required.

Graphene samples on 90 nm SiO₂ on silicon [Figs. 1(a) and 1(b)] appeared brighter than the surrounding substrate

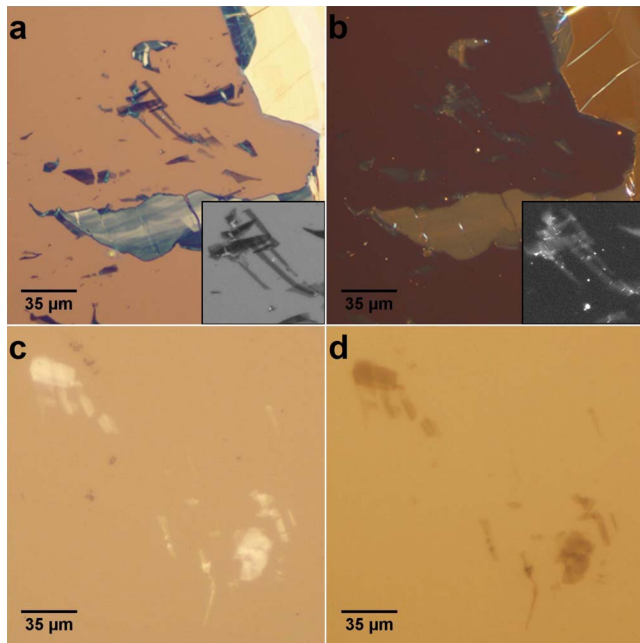


FIG. 1. (Color online) (a) Optical micrographs of graphene flakes deposited on a silicon substrate with 90 nm oxide appear dark compared to the substrate. (b) The graphene, when viewed between crossed polarizers, becomes lighter than the substrate due to the rotation of the polarized light enabling the transmitted light to pass through the second polarizer. A region containing single- and few-layer graphene shown at 550 nm illumination is shown in the insets to highlight the effect. Conversely, similar images of graphene deposited on ultraflat mica appears bright (c) due to reflectivity but appears darker when viewed through crossed polarizers (d) indicating a lack of optical activity on this substrate.

when viewed with crossed polarizers—negative contrast. If the illumination is filtered to 550 nm light, the wavelength for peak contrast on this substrate, the effect is clearly visible for even few-layer graphene as shown in the inset images. The magnitude of the contrast compared to the substrate for crossed polarizers was observed to increase with graphene thickness up to six layers, approaching the observed contrast of thick graphite on the same substrate (Fig. 2). Measurements without polarizers showed an increase in contrast with graphene layers, as has been reported on previously.^{22,23} It was also noted that folds in the graphene became highly visible against the graphene observed in reflection or transmission. Graphene deposited on ultraflat mica [Figs. 1(c) and 1(d)] showed an increase in contrast, the opposite behavior from the SiO₂ substrate. A similar effect was observed for graphene transferred back to a HOPG substrate and a highly doped (1–10 Ω cm) silicon substrate.

Graphene samples were also imaged under crossed polarizers where the sample was rotated with respect to the polarization direction of the illumination. Here no dependence on sample orientation was found with the exception of folds in the graphene. This dependence however shows a 180° periodicity, suggesting that it is a manifestation of the fold having a stronger electric dipole moment along the direction of the fold (Fig. 3).

The graphene samples were tested for circular dichroism by taking images of samples on glass, illuminated by right

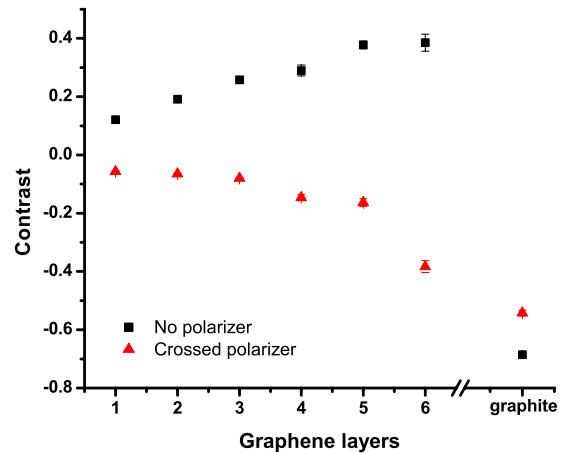


FIG. 2. (Color online) Measured contrast of graphene on 90 nm SiO₂ with crossed polarizers (▲) and without polarizers (■) as a function of the number of graphene layers. Without polarizers, the contrast is seen to increase with the thickness of graphene. Not shown on the graph is the eventual decrease in contrast with greater thickness. This ultimately results in the negative contrast of graphite due to the increasing reflectivity of thicker graphene/graphite layers. Under crossed polarizers, the graphene always has negative contrast. The lower magnitude of contrast for graphite under crossed polarizers is understood to be due to the decreased transmission of light through the crossed polarizers.

and left circularly polarized light (RCP and LCP, respectively) (Fig. 4). The $\frac{1}{4}$ wave plates used for the circular polarization filters were zero order centered on 632 nm. Regions corresponding to between one and seven layers of graphene were measured. Optical absorption was determined by measuring the intensity of light passing through the samples compared to a nearby section of clean substrate. The differential absorption was found to increase from one to three layers of graphene and thereafter remain relatively unchanged with increasing sample thickness. Samples on 90 nm oxide were also tested in this manner and found to show a nonzero CD. In contrast, samples of graphene suspended on a transmission electron microscopy grid and therefore unsupported by a substrate, did not show CD.

III. DISCUSSION

As a chiral material, it would be of interest to attempt to extract a chirality parameter, κ , for the graphene. However we would caution against such an analysis for the reason that κ is tied to the effective-medium approximation.²⁴ The effective-medium approximation does not consider the individual elements that are involved in the chirality. This analysis works very well for an active molecule dispersed in a solvent but does not make physical sense for a two-dimensional (2D) solid such as graphene.

It should be noted that the observation of CD on opaque substrates can help to further understand the nature of the optical activity. Such measurements must be done by reflection, where circularly polarized light reverses its handedness. Thus a single photon will pass through the graphene once as right and once as left-handed light. If the chiral properties

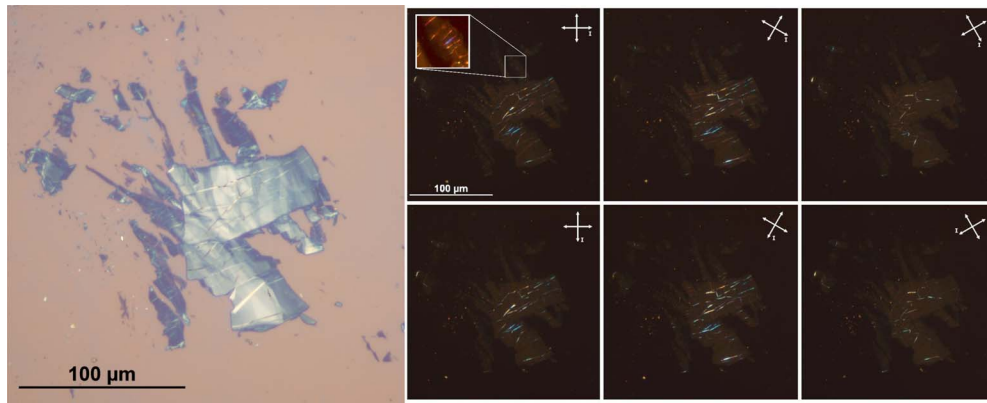


FIG. 3. (Color online) A multilayer graphene sample with folds (white light microscopy image on left) is viewed between crossed polarizers (sequence of images on right). Folds become most visible when they are oriented at 45° to the incoming and outgoing polarizers (polarization direction noted by white arrows, incoming is labeled with “I”). The effect is due to the fold having a strong electrical polarization along the direction of the fold. The folds are most visible in the thickest parts of the samples; however they remain visible even for few-layer graphene (inset in first image in the sequence on the right).

were brought about due to some interlayer effects, such as a rotation in lattice orientation between layers, the handedness of the material would be the same when viewed from either side making the differential absorption zero. However, if the chiral quality is confined to the 2D sheet of a single graphene plane, then the handedness will depend on the side from which the sample is viewed, and thus will not cancel out with reflection.

The visibility of the folds on the silicon sample may be due to coupling of the enhanced dipole moment along the direction of the fold. The incoming light is polarized along the horizontal axis of the image, and the analyzer is aligned with the vertical axis. Under these circumstances, a third linear polarizer placed in-between would have maximal transmission when it is at 45° to the other polarizers. Careful inspection shows that the folds which are oriented at angles close to 45° are the most visible while examples of folds

which are vertically or horizontally aligned are not visible.

Comparing the two causes of chirality: (1) a soft, shear mode that can couple to the substrate as a means to reduce stress, or a stiff, optical bulk mode that can couple to the folds, though occurring in opposite directions, or (2) a weak magnetic field that can cause some chirality, we expect that the first of these is by far the most likely. A soft, shear mode [Figs. 4(a) and 4(b)] would be dependent on the applied stress and could couple also, e.g., to long-range rippling and buckling of the graphene.²⁵

Cause (1) relates primarily to surface roughness of the substrate, which we feel best explains the observed differences in the strength of the effect; we observe circularly polarized reflection on SiO_2 and on glass substrates but not on doped Si. Also on ultraflat mica²⁶ (Fig. 1) and unsupported graphene the effect appears to go away. This comparison clearly indicates a certain control over optical activity via careful choice of the surface properties. Notably, the CD occurs even for a single layer, it increases for the first few subsequent layers, and finally it remains unchanged thereafter. As a result, we may partially rule out interlayer and twist deformations as a structural cause, and also the proximity of each layer to the substrate seems most important.

For optical activity, it is required that a structural distortion break at least one mirror symmetry to produce optical activity. As an example [Fig. 5(a)] the calculated normal modes from an all-neighbor tight-binding model²⁷ exhibit no net rotary, nor “twisting,” distortion in the infinite sheet but the corresponding modes in the finite ribbons [Figs. 5(b) and 5(c)] do show the possibility to break at least one mirror symmetry. Here we choose to show very narrow nanoribbons of 1–2 nm width to clearly indicate the calculated atomic displacement fields. By distorting, e.g., the central hexagons of the ribbon, these structures lose one mirror plane and, by symmetry on the substrate, would become optically active in a static distortion. The model assumes asymmetric pinning to the substrate at points to hold the static distortion in place and extrapolation to long wavelength of the soft phonon modes. For completeness, we also calculated the vibrational density of states (VDOS) at room temperature [Fig. 5(d)] via

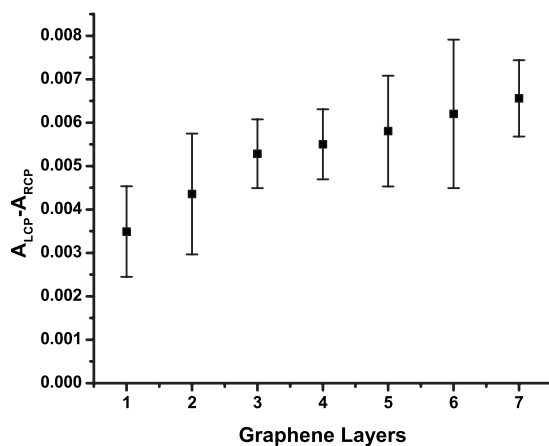


FIG. 4. Differential absorption of left and right circularly polarized light from 590 to 660 nm transmitted through a graphene sample on glass. Measurements were made on samples with thicknesses ranging from one to seven layers of graphene. Absorption is seen to increase for the first three layers and remain nearly constant for thicker samples. Thickness was determined via optical absorption and confirmed by AFM and Raman measurements.

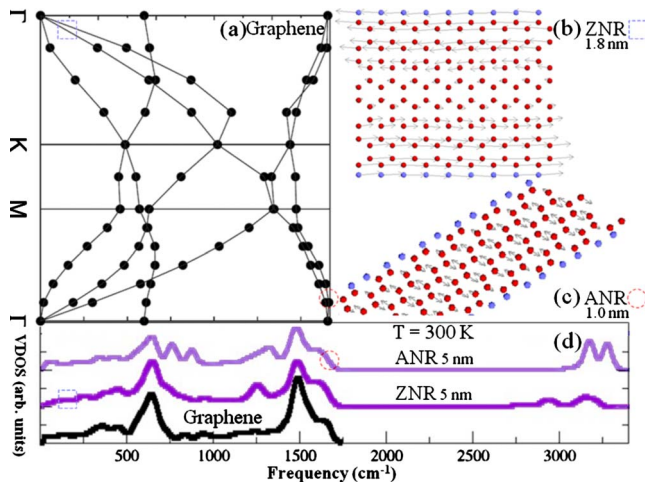


FIG. 5. (Color online) Calculated phonon dispersion of (a) ideal graphene and two related shear modes of (b) zigzag- and (c) armchair-edge nanoribbons (ZNR and ANR, respectively), which at atomic scale exhibit static (instantaneous) chiral displacements. Also shown are (d) the calculated VDOS at 300 K for (top to bottom) armchair, zigzag, and ideal graphene.

velocity autocorrelation.²⁸ We found a small upshift in frequencies and a broadening with temperature. For large samples (>5 nm), the low-frequency dispersion becomes like ideal graphene. Localized edge modes might also contribute some CD in the infrared, coupling most strongly to the high-frequency, C-H bond-stretching modes [far right in Fig. 5(d)] or to modes involving other functional groups attached to the edge.

Finally, attempts to apply a magnetic field (~ 2 kG) to the samples did not produce any change in the optical appear-

ance of samples at or above the sensitivity level of our camera. This would seem to rule out any secondary cause of optical activity, as discussed above, and we are left with structure as the primary cause of the effect. Taking this for granted, our method provides evidence that almost all exfoliated graphene samples are strained on the substrate, or alternatively, that circular dichroism provides a useful tool for identifying strained versus unstrained samples. Also, the observation of optical activity in graphene should be kept in mind when performing optical characterization given that most microscopes inadvertently impart some polarization to the light passing through if a beam splitter is incorporated into the illumination optics. In such circumstances the beam splitter can act as a weak pair of crossed polarizers and thus the intensity of light reaching the detector can be altered. Although the effect of this will be weak, it will impact precision optical measurements made on graphene.

ACKNOWLEDGMENTS

We would like to thank Anna Swan of Boston University for providing the Raman analysis of our samples and Zhiyoung Gu at UML for the use of the facilities in his laboratory for some of these experiments. We would also like to thank Alkim Akyurtlu and Nantakan Wongkasem of UML for their input on the chirality measurements and Antonio Castro-Neto from Boston University for comments on the manuscript. This work was supported by the National Science Foundation under the Nanoscale Science and Engineering Centers Program (Award No. NSF-0425826). D.F. was supported by the Office of Naval Research, via the NRL-USNA Cooperative Program.

*Author to whom correspondence should be addressed; joel_therrien@uml.edu

¹K. S. Novoselov, D. Jiang, F. Schedin, T. J. Booth, V. V. Khotkevich, S. V. Morozov, and A. K. Geim, *Proc. Natl. Acad. Sci. U.S.A.* **102**, 10451 (2005).

²A. H. Castro Neto, F. Guinea, N. M. R. Peres, K. S. Novoselov, and A. K. Geim, *Rev. Mod. Phys.* **81**, 109 (2009).

³A. K. Geim and K. S. Novoselov, *Nature Mater.* **6**, 183 (2007).

⁴B. Obradovic, R. Kotlyar, F. Heinz, P. Matagne, T. Rakshit, M. D. Giles, M. A. Stettler, and D. E. Nikonov, *Appl. Phys. Lett.* **88**, 142102 (2006).

⁵W. Hong, Y. Xu, G. Lu, C. Li, and G. Shi, *Electrochem. Commun.* **10**, 1555 (2008).

⁶J. S. Bunch, A. M. van der Zande, S. S. Verbridge, I. W. Frank, D. M. Tanenbaum, J. M. Parpia, H. G. Craighead, and P. L. McEuen, *Science* **315**, 490 (2007).

⁷I. W. Frank, D. M. Tanenbaum, A. M. Van der Zande, and P. L. McEuen, *J. Vac. Sci. Technol. B* **25**, 2558 (2007).

⁸S. Stankovich, D. Dikin, G. Dommett, K. Kohlhaas, E. Zimney, E. Stach, R. Piner, S. Nguyen, and R. Ruoff, *Nature (London)* **442**, 282 (2006).

⁹F. Schedin, A. Geim, S. Morozov, E. Hill, P. Blake, M. Katsnel-

son, and K. Novoselov, *Nature Mater.* **6**, 652 (2007).

¹⁰S. Gowtham, R. H. Scheicher, R. Ahuja, R. Pandey, and S. P. Karna, *Phys. Rev. B* **76**, 033401 (2007).

¹¹N. Varghese, U. Mogera, A. Govindaraj, A. Das, P. Maiti, A. Sood, and C. Rao, *ChemPhysChem* **10**, 206 (2009).

¹²K. S. Kim, Y. Zhao, H. Jang, S. Y. Lee, J. M. Kim, K. S. Kim, J. H. Ahn, P. Kim, J. Y. Choi, and B. H. Hong, *Nature (London)* **457**, 706 (2009).

¹³Z. Q. Li, E. A. Henriksen, Z. Jiang, Z. Hao, M. C. Martin, P. Kim, H. L. Stormer, and D. N. Basov, *Nat. Phys.* **4**, 532 (2008).

¹⁴R. R. Nair, P. Blake, A. N. Grigorenko, K. S. Novoselov, T. J. Booth, T. Stauber, N. M. R. Peres, and A. K. Geim, *Science* **320**, 1308 (2008).

¹⁵F. Wang, Y. Zhang, C. Tian, C. Girit, A. Zettl, M. Crommie, and Y. R. Shen, *Science* **320**, 206 (2008).

¹⁶K. F. Mak, M. Sfeir, Y. Wu, C. H. Lui, J. Misewich, and T. Heinz, *Phys. Rev. Lett.* **101**, 196405 (2008).

¹⁷A. B. Kuzmenko, E. Heumen, F. Carbone, and D. Marel, *Phys. Rev. Lett.* **100**, 117401 (2008).

¹⁸J. Applequist, *Am. Sci.* **75**, 58 (1987).

¹⁹A. D. Buckingham and P. J. Stephens, *Annu. Rev. Phys. Chem.* **17**, 399 (1966).

- ²⁰K. S. Novoselov, A. K. Geim, S. V. Morozov, D. Jiang, Y. Zhang, S. V. Dubonos, I. V. Grigorieva, and A. A. Firsov, *Science* **306**, 666 (2004).
- ²¹A. C. Ferrari, J. C. Meyer, V. Scardaci, C. Casiraghi, M. Lazzeri, F. Mauri, S. Piscanec, D. Jiang, K. S. Novoselov, S. Roth, and A. K. Geim, *Phys. Rev. Lett.* **97**, 187401 (2006).
- ²²C. Casiraghi, A. Hartschuh, E. Lidorikis, H. Qian, H. Harutyunyan, T. Gokus, K. S. Novoselov, and A. C. Ferrari, *Nano Lett.* **7**, 2711 (2007).
- ²³P. Blake, E. Hill, A. Castro Neto, K. Novoselov, D. Jiang, R. Yang, T. Booth, and A. Geim, *Appl. Phys. Lett.* **91**, 063124 (2007).
- ²⁴I. V. Lindell, A. H. Sihvola, S. A. Tretyakov, and A. J. Viitanen, *Electromagnetic waves in chiral and bi-isotropic media* (Artech House, Norwood, MA, 1994).
- ²⁵A. Fasolino, J. H. Los, and M. I. Katsnelson, *Nature Mater.* **6**, 858 (2007).
- ²⁶C. H. Lui, L. Liu, K. F. Mak, G. W. Flynn, and T. F. Heinz, *Nature (London)* **462**, 339 (2009).
- ²⁷D. Finkenstadt, G. Pennington, and M. J. Mehl, *Phys. Rev. B* **76**, 121405(R) (2007).
- ²⁸D. Finkenstadt, N. Bernstein, J. L. Feldman, M. J. Mehl, and D. A. Papaconstantopoulos, *Phys. Rev. B* **74**, 184118 (2006).